Single-Stage Switched-Resonator Converter Topology with Wide Conversion Ratio for Volume-Sensitive Applications

Alon Cervera, *Student Member, IEEE,* Shmuel (Sam) Ben-Yaakov, *Fellow, IEEE*,
and Mor Mordechai Peretz, *Member, IEEE*
The Center for Power Electronics and Mixed-Signal IC, Department of Electrical and Computer Engineering
Ben-Gurion University of the Negev, P.O. Box 653, Beer-Sheva, 8410501 Israel
cervera@bgu.ac.il, sby@bgu.ac.il, morp@ee.bgu.ac.il
http://www.ee.bgu.ac.il/~pemic

***Abstract*— In this study, a switched-resonator converter with high efficiency over a wide conversion ratio range is introduced. Inspired by the gyrator resonant switched-capacitor concept, the new topology provides high efficiency over wide and continuous range of conversion ratios using a single resonator. This is enabled by new modes of operation (switching sequences) developed and analyzed in this study, that modifies the charge-balance of the flying capacitor. By that, the efficiency characteristics of the converter can be shaped to peak at various conversion ratios. A generalized methodology is presented to describe resonator-type converters with multiple operation-modes as two-ports, which is then used to analyze three showcase operational modes of the presented topology. Experimental results of the three modes validate the developed theoretical model, and demonstrate the superiority of the concept in terms of efficiency (over 10%) and current-sourcing capabilities (over 80%) using a compact 5W prototype.**

***Keywords*— switch-mode converters; switched-capacitor converter; gyrator; efficiency; switched-resonator converters**

I. INTRODUCTION

Switched capacitor converters (SCCs) have limited capabilities for voltage regulation due to the tight relationship between the voltage gain and the converter efficiency [1-10]. In such converters, the efficiency is linearly tied to the ratio between the output voltage and target voltage (the no load SCC output voltage, V_{out} / V_{target}) which stems from the rigid proportionality between the input and output charges [1-10].

Regulation can be achieved either by varying the SCC parameters [1,11,12], or by inserting a post regulation stage [13-15] to match the required conversion ratio. Another possible approach for voltage regulation by SCC is to generate multiple target voltages using multiple flying-capacitor cells and therefore increase the effective operation range [1,16-20]; the system efficiency however, would remain of a discrete nature.

To reduce switching losses, allow higher operating frequency and reduce the total volume of the converters, various derivatives of resonant-type SCC (RSCC) have been employed [21-29]. Since the operation of RSCCs is similar to the conventional SCCs in the sense that similar switching sequences are applied, the efficiency of the converter is still strongly dependent on the voltage gain. As a result, the challenge of regulating the output remains, i.e. to produce an output voltage that is different than the target voltage still requires adding losses in series to the converter [1,30-33]. The reason for that is when the output voltage is different from the target voltage, the charge-balance of the flying capacitor(s) is not satisfied [9,34,35], affecting the average current. In such case, the converter's operating point shifts till the voltage drop across the parasitic series resistances matches the difference between the output and target voltages.

More sophisticated approaches to facilitate voltage regulation without losses introduced an additional, charge/discharge path, i.e. additional switching state or states, to satisfy the capacitor charge-balance. This has been adopted in several previous studies by either internally circulating residual charge [36], by working above resonant frequency to exhibit inductive behavior (partially losing soft-switching capabilities) [37,38], or by combining resonant and linear operation to completely deplete the residual charge in every switching cycle [34-41].

A recently-developed gyrator mode resonant switched-capacitor converter (GRSCC) presented in [34,42,43] has demonstrated a unique potential for efficient voltage regulation over a wide range of conversion ratios. The main attribute of the GRSCC is that it disengages the efficiency of the system from the voltage gain. This is achieved by introducing an additional switching phase to balance the mismatch between the input and the output average currents. As a result, the conventional SCC topology is transformed into a voltage-dependent current source, i.e. a gyrator-like converter [44-47]. GRSCC exhibits continuous gain that can be controlled by pulse-density modulation (PDM) [48,49]. Nevertheless, high conversion ratios in this topology remain problematic due to the large mismatch between the input and output current, which translates into

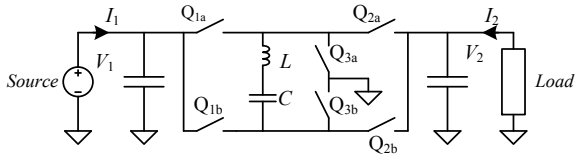

Fig. 1 The presented multi-mode switched-resonator converter.

a high circulating current. This is overcome in the presented new family of converters, the *switched-resonator converters* (SwRCs), by introducing additional switching states. This new method of operation enables *disengagement of the system's efficiency from the voltage gain*. A feature resided thus far in switched-inductor converters. Nonetheless, since these converters share a similar hardware configuration with their precursors, they still retain the volume benefits.

The objective of this study is to introduce a new SwRC with high-efficiency over a wide range of conversion ratios and present a unique methodology to shape the efficiency characteristics of the converter by the switching scheme. The primary advantage of this converter is that wide and continuous conversion ratio with high efficiency is achieved using a single energy transfer cell (i.e., one flying capacitor). This allows ultimate volume and complexity reduction when compared to other multi-target voltage converters that employ switched-capacitor [16-18] or switched-resonant approaches [20]. A further objective of this research is to develop a generalized methodology to describe resonator-type converters with multiple operation-modes as two-port networks. Three operation modes (switching schemes of the converter) are demonstrated as a showcase of power-sourcing and efficiency capabilities of the new converter.

The converter in its simplistic form, shown in Fig. 1, is a modification of a soft-switched resonant SCC with switch assembly inspired by multi-target voltage converters such as the binary/Fibonacci SCC [17,20] or the GTSP [16,18]. As opposed to other configurations that employ multiple flying tanks, in this study a single energy-transfer cell is used. The switches configuration allows the resonator to connect the input or the output ports directly or with reverse polarity, as well as a series-parallel connection to either port. By that, multiple switching possibilities to achieve charge balance of the tank can be realized. As demonstrated previously in [34,42,43], this is an enabler to disengage the rigid relationship between the efficiency and the voltage gain.

The rest of the paper is organized as follows: Section II provides a general analysis for an LC switched-resonator converter as a two-port network. Section III delineates three operation modes of the presented converter with analysis to compare performance. Experimental results are provided in Section IV. Section V concludes the paper.

II. Generalized Conversion Characteristics of a Switched-Resonator Network as a Two-Port

A switch-mode converter can be described as a two-port network, as illustrated in Fig. 2, using average and dynamic behavioral modeling [42] to define a relationship between the input and output port voltages V_1, V_2, and currents I_1, , I_2. Two parameters are considered known and independent, while the dependency of the rest can be defined by the admittance, that is:

$$\begin{bmatrix} I_1 \\ I_2 \end{bmatrix} = \begin{bmatrix} Y_{11} & Y_{12} \\ Y_{21} & Y_{22} \end{bmatrix} \begin{bmatrix} V_1 \\ V_2 \end{bmatrix} . \qquad (1)$$

The matrix parameters Y_{11} and Y_{22} represent the ports' self-admittance, i.e. dependence of each port's current on its own voltage, while Y_{12} and Y_{21} give the cross-admittances. A matrix where $Y_{12} = G$, $Y_{21} = -G$ and $Y_{11} = Y_{22} = 0$, describes an ideal *gyrator* element [45].

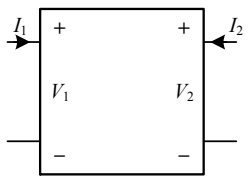

Fig. 2 Two-port

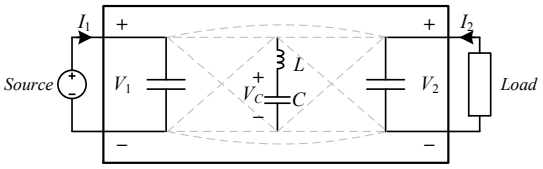

Fig. 3 A view of a switched-resonator network with dashed-lines signifying possible connection routes to the input and output ports.

A. Two-Port Admittance Modelling of a Switched-Resonator Network

Consider a generalized switched-resonator converter, illustrated in Fig. 3 with average port voltages V_1, V_2, and a switch assembly that applies N combinations of V_1 and V_2, i.e. *states*, on the resonator network of L and C. A soft-switching mechanism that is employed, assures transition between states at zero current after half-resonance period. Since the resonant behavior in each state is of a 2nd order, the converter can be analyzed in a discrete form by viewing the potential applied on the tank (resonator) during the state's interval and determining the values at the end of each state.

The tank's capacitor voltage at the end of state n, namely $V_{C,n}$, can be derived from its initial condition, $V_{C,n-1}$, and the voltage that is applied on the tank at the specific state, E_n. Assuming high resonant quality-factor, i.e. negligibly small losses, $V_{C,n}$ can be expressed at the half-resonance switching-point as:

$$V_{C,n} \approx 2E_n - V_{C,n-1} \quad , \quad E_n = f\left(V_1, V_2\right) . \qquad (2)$$

Populating the values for E_n into (2) for each of the states gives N equations with N unknowns $V_{C,1}$ to $V_{C,N}$. Assuming that all equations are independent, a unique solution exists with all the unknowns a function of V_1 and V_2, i.e. the steady-state values for $V_{C,1}$ to $V_{C,N}$ are fixed and known. It should be noted that some switching combinations may result in dependent equations or diverged solutions. These cases are beyond the scope of this paper and will be addressed in subsequent publications.

The average current value in each state, $I_{C,n}$, is derived from the total charge difference from the previous state, that is:

$$I_{C,n} \approx \frac{2C}{T_{state}}\left(V_{C,n} - V_{C,n-1}\right) \quad , \quad T_{state} = \pi\sqrt{LC} \qquad (3)$$

where L and C are the inductance and capacitance of the resonator, respectively. Once $I_{C,n}$ is obtained for the complete sequence, I_2 can be derived by averaging all the state currents throughout the cycle in which the resonator connects to the output node. I_1 is derived in a similar manner. This yields:

$$\begin{aligned} I_1 &= F\,T_{state} \sum_{n=1}^{N} x_n I_{C,n} \quad , \quad x_n \in \{-1,0,1\} \\ I_2 &= F\,T_{state} \sum_{n=1}^{N} y_n I_{C,n} \quad , \quad y_n \in \{-1,0,1\} \end{aligned} , \qquad (4)$$

where F is limited by the repetition rate of the cycle, i.e. the frequency for the sum of switching states that compose one cycle $F \le F_{max} = (N T_{state})^{-1}$, and x_n, y_n are constants which indicate whether the tank is connected to the input and/or output at state n as well as the connection polarity. Current regulation can be obtained by modifying F with pulse-density modulation techniques [42], affecting the result of (4).

Since (2)-(4) can be rewritten as a function of V_1 , V_2, after some manipulation (4) can be expressed as a function of the admittances as:

$$I_1 = Y_{11}V_1 + Y_{12}V_2 \Big| \quad I_2 = Y_{21}V_1 + Y_{22}V_2 \ , \tag{5}$$

i.e. depends entirely on L, C and F

B. Efficiency Modelling

The efficiency of the converter can be obtained by evaluating the losses P_{loss} and the output power P_{load}, which form:

$$\eta = \left[1 + P_{loss}/P_{load}\right]^{-1} \ . \tag{6}$$

P_{loss} is obtained by summing the individual losses created in each state. Assuming no other significant losses thanks to the ZCS, the losses are due to the rms currents $I_{C,n,rms}$, through the conduction path resistance R. The total power dissipation can then be obtained using (3), with the average-to-rms ratio for a sine wave as:

$$P_{loss} = R\sum_{n=1}^{N} {I_{C,n,rms}}^2 \approx F\,T_{state} R \frac{\pi^2}{8} \sum_{n=1}^{N} {I_{C,n}}^2 \ , \tag{7}$$

where R is assumed here identical for all states without loss of generality. The expression of (7) can be rewritten in a general form, represented by basic parameters from (2), (3):

$$P_{loss} = \frac{F R C^2}{T_{state}} \left(\alpha {V_1}^2 + \beta {V_2}^2 - \gamma V_1 V_2 \right) \ , \tag{8}$$

where the constants α, β, γ are weighting-factors of V_1 , V_2 based on the mode of operation.

The output power can also be directly expressed by V_1 and V_2 and the parameters of the converter's admittance (5) . This yields:

$$P_{load} = -P_2 = -\left(Y_{21} V_2 V_1 + Y_{22} {V_2}^2 \right). \tag{9}$$

In cases where the loss contribution of Y_{22} is relatively small, (8) and (9) can be substituted into (6) to form an efficiency expression that depends directly on the conversion ratio, A:

$$\eta = \left[1 + B\left(\alpha A^{-1} + \beta A - \gamma \right) \right]^{-1}, \ A = \frac{V_2}{V_1} \ , \tag{10}$$

where B combines the independent parameters from (8) and (9). It can be seen from (10) that as described in [34], the efficiency variation of the switched-resonator network described here depends on the conversion ratio alone.

Taking the derivative of (10) and equating to zero yields the conversion ratio in which the peak efficiency can be achieved, that is:

$$A_{optimal} = A\big|_{\max(\eta)} = \sqrt{\frac{\alpha}{\beta}} \ . \tag{11}$$

This implies that, assuming operation under ZCS and that the resonator is switched periodically after half-resonance, the location of the peak efficiency point is a weighted-function of the ports' voltages and can be adjusted by the applied voltage on the resonator, i.e. by modifying the switching sequence. This provides a new design direction and guideline for SCCs and their derivatives, as will be shown next, enabling to shift the rigid optimal target voltage by manipulating the applied voltage on the energy-transfer cell.

III. Wide- Conversion Ratio Operation Modes

The switched-resonator topology presented in Fig. 1 includes seven possible switching states delineated in Fig. 4 as states S_A-S_G, in which the resonator may be subjected to the following potentials:

$$\begin{matrix} E_A = V_1 & E_C = -V_1 & E_E = V_1 - V_2 \\ E_B = V_2 & E_D = -V_2 & E_F = V_2 - V_1 \end{matrix} \quad E_G = 0 \tag{12}$$

To showcase the flexibility of adjusting the peak efficiency point to target operating conditions, three modes of operation are presented. A key factor in defining a switching sequence is to assure that charge balance of the flying capacitor is maintained within a cycle. The operation modes, i.e. the voltages that are applied on the resonator per state, are chosen such that the capacitor voltage at the end of a switching sequence resumes its initial values. This condition is satisfied if a solution to (2) exists. The new operation modes of this study are defined with respect to the method in which the voltage is applied on the resonator, and compared to a bridge variation of the GRSCC with optimal conversion ratio of $A \approx 0.58$ [50,51] as a benchmark. Typical waveforms of the operation modes are depicted in Fig. 5, and the calculated conversion and efficiency characteristics of the operation modes are summarized in Table I.

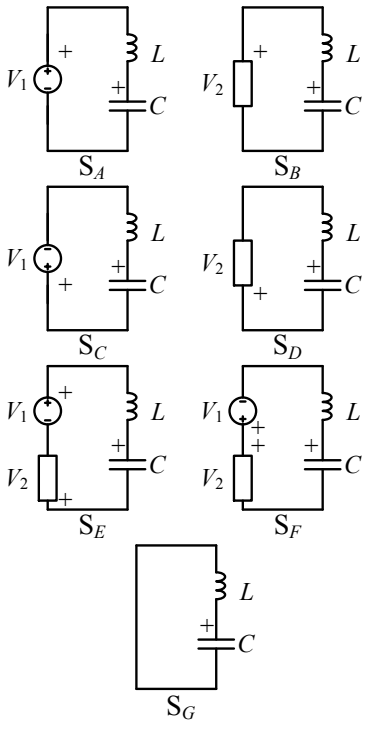

Fig. 4 Possible connection states for the converter presented in Fig. 1. Active switches for the various states. . S_A: Q_{1a}, Q_{3b}; S_B: Q_{2a}, Q_{3b}; S_C: Q_{3a}, Q_{1b}; S_D: Q_{3a}, Q_{2b}; S_E: Q_{1a}, Q_{2b}; S_F: Q_{2a}, Q_{1b}; S_G: Q_{2a}, Q_{2b}

A benchmark operation mode is the case of a bridge GRSCC configuration. In this mode [see Fig. 5(a)], namely **bridge mode** [50,51], the resonator is subjected to the voltage difference between the input and the output [i.e. S_E, see Fig. 4] to charge the flying capacitor, it is then followed by S_B that applies the output voltage on the resonator. Finally, charge balance is achieved by a short-circuit [S_G, Fig. 4].

In the **semi-complementary mode** [Fig. 5(b)], charge balance is facilitated through a different switching sequence. In the charge state S_E the resonator is subjected to $V_1 - V_2$. Then, by applying S_B, the network connects to V_2 and charge is transferred to the output. Charge balance is achieved in this mode through state S_D which applies a negative voltage ($-V_2$).

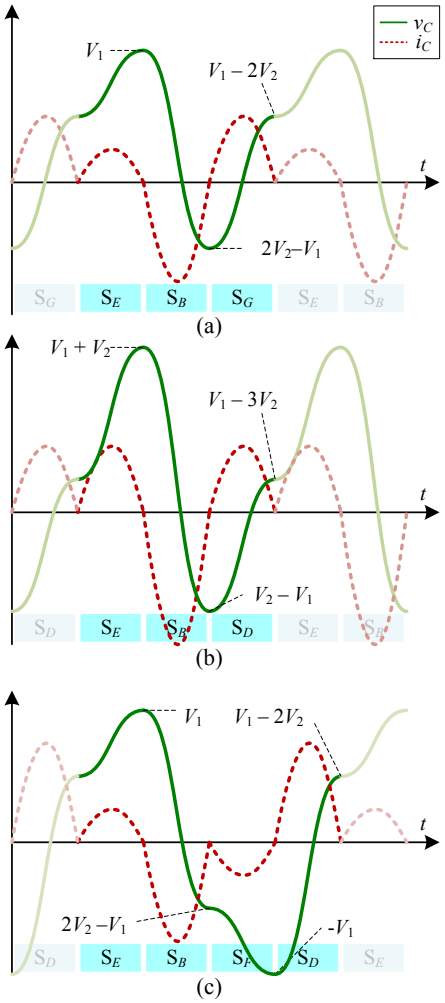

Fig. 5 Example waveforms of the presented converter when $V_1 = 4V_2$ for the following modes: (a) bridge-GRSCC; (b) semi-complementary; (c) complementary.

In the **complementary mode** [Fig. 5(c)], symmetric positive and negative voltages are applied on the resonator to achieve charge balance. By initiating S_E, the resonator is subjected to $V_1 - V_2$ and charges. Then it is subjected to V_2 to discharge by applying state S_B. To maintain charge balance the resonator is then inversely charged by S_F that subjects it to the negative potential $-(V_1 - V_2)$, and then discharged by S_D which applies the negative voltage ($-V_2$).

Comparison between the modes of operation in Table I reveals several differences in the properties of the new converters. It can be observed that although identical conditions are applied in terms of the ports' voltages and components values, the resultant admittance matrices of the new modes are double than in the bridge configuration. This directly translates to increased current sourcing capability of the converter. The semi-complementary mode is capable of outputting twice the power than the bridge-GRSCC for the same conditions (frequency and R, L values), complementary mode output power capability is increased by factor of 1.5 since the frequency limit is different.

Another important property difference can be found in the efficiency as a function of the conversion ratio A. The expressions from Table I for the efficiency have been plotted for better view and are presented in Fig. 6 for all modes. In Fig. 6(a) a case in which equal resonator parameters are used for all modes is depicted. It can be seen that for the majority of conversion ratios the converter is most efficient when using the complementary mode, with peak efficiency at $A = 0.71$. In Fig. 6(b), the resonator's parameters are adapted such that admittance matrix values are the same for all modes, i.e. for the same power delivery capability. It can be seen that both modes are distinctively more efficient than the conventional bridge configuration. It can also be seen that each of the modes has a region of efficiency where it is more efficient than the other; $A = 0.3$ marks the boundary point.

IV. Experimental Verification

To demonstrate the operation of the various modes of the switched-resonator converter and to validate the theoretical analysis, a low output-voltage prototype was built and tested; $V_1 = 5$V to $V_2 = 1.2$V. The prototype was tested for the three operation modes described earlier. Experimental waveform of the resonator's current and the capacitor's voltage operating in steady-state are shown in Fig. 7; the resonator's parameters were $C = 220$nF,

TABLE I: Performance Characteristics

	***Bridge* [50,51]**	***Semi-complementary***	***Complementary***
F_{max}	$\left(3\pi\sqrt{LC}\right)^{-1}$	$\left(3\pi\sqrt{LC}\right)^{-1}$	$\left(4\pi\sqrt{LC}\right)^{-1}$
Voltages	$\begin{cases} V_{C,1} \approx V_1 \\ V_{C,2} \approx 2V_2 - V_1 \\ V_{C,3} \approx V_1 - 2V_2 \end{cases}$	$\begin{cases} V_{C,1} \approx V_1 + V_2 \\ V_{C,2} \approx V_2 - V_1 \\ V_{C,3} \approx V_1 - 3V_2 \end{cases}$	$\begin{cases} V_{C,1} \approx V_1 \\ V_{C,2} \approx 2V_2 - V_1 \\ V_{C,3} \approx -V_1 \\ V_{C,4} \approx V_1 - 2V_2 \end{cases}$
Admittance	$\begin{bmatrix} 0 & 2FC \\ -2FC & 0 \end{bmatrix}$	$\begin{bmatrix} 0 & 4FC \\ -4FC & 0 \end{bmatrix}$	$\begin{bmatrix} 0 & 4FC \\ -4FC & 0 \end{bmatrix}$
Efficiency	$\left[1 + \frac{\pi R}{2\sqrt{L/C}}\left(A^{-1} + 3A - 3\right)\right]^{-1}$	$\left[1 + \frac{\pi R}{4\sqrt{L/C}}\left(A^{-1} + 4A - 3\right)\right]^{-1}$	$\left[1 + \frac{\pi R}{4\sqrt{L/C}}\left(A^{-1} + 2A - 2\right)\right]^{-1}$
Optimal conversion ratio	0.58	0.5	0.71

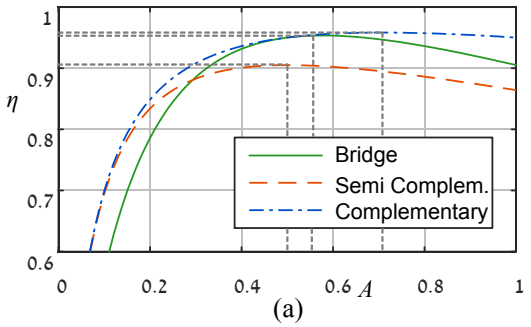

(a)

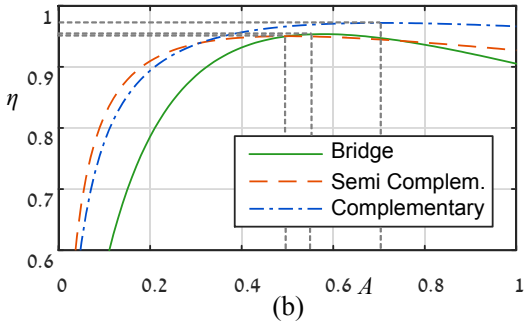

(b)

Fig. 6 Theoretically calculated efficiency plots of the presented converter as a function of conversion ratio for the three presented operating modes when: (a) R,L,C are the same in all topologies; (b) Resonator impedance is equal for all modes. Efficiency peaks are marked by dashed vertical lines.

$L \approx 40$nH ($T_{state} = 300$ns). The differences between the modes are apparent. The output power of the bridge-GRSCC was measured 2.75W, for the complementary mode 3.9W and for the semi-complementary 5.1W. These results are in excellent agreement with the theoretical prediction from Table I.

Fig. 8 shows the efficiency as a function of the conversion ratio for all three modes. These measurements were carried out using an electronic load that was programmed to sweep V_2. The cycle frequency of the converters was set to maximum - F_{max}, i.e. maximizing the power output capability at each of the modes. As can be seen, a very good agreement is obtained with the theoretical curves of Fig. 6. Also demonstrated is the different conversion ratio for the peak efficiency at each of the modes.

V. Conclusion

A new switched-resonator converter with several possible modes of operation has been presented and demonstrated efficiency characteristics that exhibit a broad peak over an extended voltage gain-range. The capability to shape the efficiency characteristics of the converter has been demonstrated as well. This attribute, *resided thus far only in multi-target voltage converters that employ several energy-transfer cells*, realized in this work by a single energy transfer cell.

A generalized procedure to describe switched-resonator or resonant-type switched-capacitor converters with multiple operation-modes as two-port networks has been described to evaluate and quantify the characteristics of such converters in various conditions. Three operation modes have been demonstrated and evaluated both theoretically end experimentally, providing different power-sourcing and efficiency capabilities. Experimental results demonstrate an increase of over 10% in efficiency at high conversion ratios compared the previously presented Bridge-GRSCC.

Combining the benefits of the relatively simple converter design and the need for a single energy-transfer cell to allow continuous high-efficiency conversion ratios, the GRSCC-based voltage regulator can be considered as an attractive candidate for voltage regulation applications that require high response rate. Furthermore, the possibility of multiple operation modes allows flexibility in the converter design and further size reduction of the resonator.

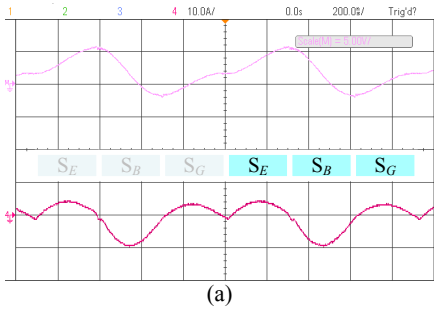

(a)

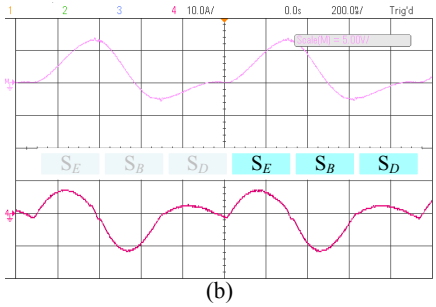

(b)

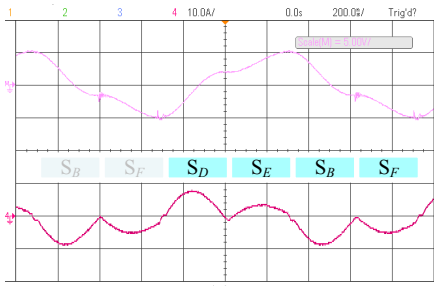

(c)

Fig. 7 Experimental waveforms of the presented converter for the following modes showing vC at the top and iC at the bottom of each screenshot: (a) bridge-GRSCC; (b) semi-complementary; (c) complementary.

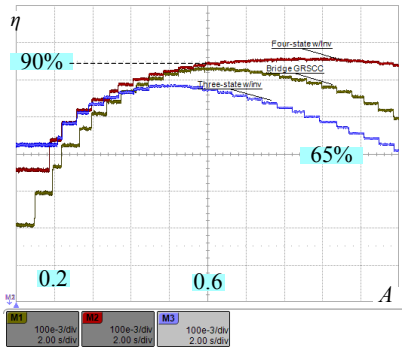

Fig. 8 Experimental efficiency sweep of the three modes as a function of output voltage gain. Vertical: 10%/Div. ; Horiz.: 0.1/Div.

VI. REFERENCES

[1] M. S. Makowski and D. Maksimovic, "Performance limits of switched-capacitor dc-dc converters," IEEE Power Electronics Specialists Conference, vol. 2, pp. 1215-1221, 1995.

[2] M. Budaes and L. Goras, "Burst mode switching mechanism for an inductorless dc-dc converter," *CAS International Semiconductor Conference*, vol. 2, pp.463-466, 2007.

[3] M. D. Seeman and S. R. Sanders, "Analysis and optimization of switched capacitor dc-dc converters," *IEEE Transactions on Power Electronics,* vol. 23, no. 2, pp. 841-851, 2008.

[4] S. Ben-Yaakov and M. Evzelman, "Generic and unified model of switched capacitor converters," *IEEE Energy Conversion Congress and Exposition,* pp. 3501-3508, 2009.

[5] J. M. Henry and J. W. Kimball, "Practical performance analysis of complex switched-capacitor converters," *IEEE Transactions on Power Electronics*, vol. 26, no. 1, pp. 127-136, 2011.

[6] S. Ben-Yaakov, "On the influence of switch resistances on switched capacitor converters losses," *IEEE Transactions on Industrial Electronics, Letters*, vol. 59, no. 1, pp. 638-640, 2012.

[7] J. M. Henry and J. W. Kimball, "Switched-capacitor converter state model generator," *IEEE Transactions on Power Electronics*, vol.27, no.5, pp.2415-2425, 2012.

[8] P. K. Peter and V. Agarwal, "On the input resistance of a reconfigurable switched capacitor dc–dc converter-based maximum power point tracker of a photovoltaic source," *IEEE Transactions on Power Electronics*, vol. 27, no. 12, pp. 4880-4893, 2012.

[9] M. Evzelman and S. Ben-Yaakov, "Average-current based conduction losses model of switched capacitor converters," *IEEE Transactions on Power Electronics,* vol. 28, no. 7, pp. 3341-3352, 2013.

[10] B. Wu, L. Wang, L. Yang, K. Smedley, and S. Singer, "comparative analysis of steady-state models for switched capacitor converter," *IEEE Transactions on Power Electronics*, *Early Access,* vol. PP, no. 99, pp. 1-1, 2016.

[11] H. S. H. Chung, "Development of DC/DC regulators based on switched-capacitor circuits," *IEEE International Symposium on Circuits and Systems,* pp. 210-213 vol. 5, 1999.

[12] M. Evzelman and R. Zane, "Burst mode control and switched-capacitor converters losses," *IEEE Applied Power Electronics Conference and Exposition,* pp. 1603-1607, 2016.

[13] S. Ben-Yaakov and A. Kushnerov, "Algebraic foundation of self adjusting switched capacitors converters," *IEEE Energy Conversion Congress and Exposition,* pp. 1582-1589, 2009.

[14] R. C. N. Pilawa-Podgurski, D. M. Giuliano, and D. J. Perreault, "Merged two-stage power converter architecture with soft charging switched-capacitor energy transfer," *IEEE Power Electronics Specialists Conference*, pp. 4008-4015, 2008.

[15] S. Lim, J. Ranson, D. M. Otten, and D. J. Perreault, "Two-stage power conversion architecture for an LED driver circuit," *IEEE Applied Power Electronics Conference and Exposition,* pp. 854-861, 2013.

[16] Y. Beck and S. Singer, "Capacitive transposed series-parallel topology with fine tuning capabilities," *IEEE Transactions Circuits Systems I, Regular Papers*, vol. 58, no. 1, pp. 51-61, 2011.

[17] A. Kushnerov and S. Ben-Yaakov, "Unified algebraic synthesis of generalized fibonacci switched capacitor converters," *IEEE Energy Conversion Congress and Exposition,* pp. 774-778, 2012.

[18] Y. Beck, S. Singer, and L. M. Salamero, "Modular realization of capacitive converters based on general transposed series-parallel and derived topologies," *IEEE Transactions Industrial Electronics*, vol. 61, no. 3, pp. 1622-1631, 2014.

[19] L. G. Salem and P. P. Mercier, "A recursive switched-capacitor dc-dc converter achieving 2^{N-1} ratios with high efficiency over a wide output voltage range," *IEEE Journal of Solid-State Circuits*, vol. 49, no. 12, pp. 2773-2787, 2014.

[20] E. Hamo, A. Cervera, and M.M. Peretz, "Multiple conversion ratio resonant switched-capacitor converter with active zero current detection," *IEEE Transactions on Power Electronics*, vol. 30, no. 4, 2073-2083, 2015.

[21] Y.-S. Lee, Y.-Y. Chiu, and M.-W. Cheng, "ZCS switched-capacitor bi-directional quasi-resonant converters," *IEEE International Conference on Power Electronics and Drive Systems,* pp. 866-871, 2005.

[22] Y.-S. Lee and Y.-P. Ko, "Switched-capacitor bi-directional converter performance comparison with and without quasi-resonant zero-current switching," *IET Power Electronics*, vol. 3, no. 2, pp. 269-278, 2010.

[23] M. Shoyama, T. Naka, and T. Ninomiya, "Resonant switched-capacitor converter with high efficiency," *IEEE Power Electronics Specialists Conference,* vol. 5, pp. 3780-3786, 2004.

[24] Y. P. B. Yeung, K. W. E. Cheng, S. L. Ho, K. K. Law, and D. Sutanto, "Unified analysis of switched-capacitor resonant converters," *IEEE Transactions on Industrial Electronics*, vol. 51, no. 4, pp. 864-873, 2004.

[25] A. Ioinovici, H. S. H. Chung, M. S. Makowski, and C. K. Tse, "Comments on 'Unified analysis of switched-capacitor resonant converters'," *IEEE Transactions on Industrial Electronics*, vol. 54, no. 1, pp. 684-685, 2007.

[26] O. Keiser, P. K. Steimer, and J. W. Kolar, "High power resonant switched-capacitor step-down converter," *IEEE Power Electronics Specialists Conference,* pp. 2772-2777, 2008.

[27] D. Cao and F. Z. Peng, "Multiphase multilevel modular dc–dc converter for high-current high-gain teg application," *IEEE Transactions on Industry Applications*, vol. 47, no. 3, pp. 1400-1408, 2011.

[28] D. Cao and F. Z. Peng, "Zero-current-switching multilevel modular switched-capacitor dc–dc converter," *IEEE Transactions on Industry Applications*, vol. 46, no. 6, pp. 2536-2544, 2010.

[29] D. Cao, S. Jiang, and F. Z. Peng, "Optimal design of multilevel modular switched-capacitor dc-dc converter," *IEEE Energy Conversion Congress and Exposition*, pp. 537-544, 2011.

[30] G. Zhu and A. Ioinovici, "Switched-capacitor power supplies: dc voltage ratio, efficiency, ripple, regulation," *IEEE International Symposium on Circuits and Systems, 1996*, Atlanta, GA, , pp. 553-556, 1996.

[31] H. S. Chung, A. Ioinovici, and Wai-Leung Cheung, "Generalized structure of bi-directional switched-capacitor DC/DC converters," *IEEE Transactions on Circuits and Systems I: Fundamental Theory and Applications*, vol. 50, no. 6, pp. 743-753, 2003.

[32] M. D. Seeman, V. W. Ng, H. P. Le, M. John, E. Alon, and S. R. Sanders, "A comparative analysis of switched-capacitor and inductor-based dc-dc conversion technologies," *IEEE Workshop on Control and Modeling for Power Electronics*, pp. 1-7, 2010.

[33] Y. Lei and R. C. N. Pilawa-Podgurski, "A General Method for Analyzing Resonant and Soft-Charging Operation of Switched-Capacitor Converters," *IEEE Transactions on Power Electronics*, vol. 30, no. 10, pp. 5650-5664, 2015.

[34] A. Cervera, M. Evzelman, M. M. Peretz, and S. Ben-Yaakov, "A high efficiency resonant switched capacitor converter with continuous conversion ratio," *IEEE Transactions on Power Electronics,* vol. 30, no. 3, 1373-1382, 2015.

[35] R. Beiranvand, "Analysis of a switched-capacitor converter above its resonant frequency to overcome voltage

regulation issue of resonant SCCs," *IEEE Transactions on Industrial Electronics*, vol. 63, no.9, pp. 5315-5325, 2016.
[36] D. Qiu and B. Zhang, "Analysis of step-down resonant switched capacitor converter with sneak circuit state," *IEEE Power Electronics Specialists Conference,* pp. 1-5, 2006.
[37] K. Sano and H. Fujita, "A resonant switched-capacitor converter for voltage balancing of series-connected capacitors," *International Conference on Power Electronics and Drive Systems*, pp. 683-688, 2009.
[38] K. Sano and H. Fujita, "Performance of a high-efficiency switched-capacitor-based resonant converter with phase-shift control," *IEEE Transactions on Power Electronics*, vol. 26, no. 2, pp. 344-354, 2011.
[39] K.-H. Liu, R. Oruganti, and F. C. Lee, "Resonant switches-Topologies and characteristics," *IEEE Power Electronics Specialists Conference,* pp. 106-116, 1985.
[40] M. Jabbari, "Unified analysis of switched-resonator converters," *IEEE Transactions on Power Electronics*, vol. 26, no. 5, pp. 1364-1376, 2011.
[41] S. Sharifi and M. Jabbari, "Family of single-switch quasi-resonant converters with reduced inductor size," *IET Power Electronics*, vol. 7, no. 10, pp. 2544-2554, 2014.
[42] A. Cervera and M. M. Peretz, "Resonant switched-capacitor voltage regulator with ideal transient response," *IEEE Transactions on Power Electronics,* vol. 30, no. 9, 4943-4951, 2015.
[43] A. Cervera and M. M. Peretz, "Envelope tracking power supply for volume-sensitive low-power applications based on a resonant switched-capacitor converter," *IEEE Applied Power Electronics Conference and Exposition*, pp. 2298-2303, 2016.
[44] B. D. Tellegen, "The gyrator, a new electric network element," *Philips Research Laboratories, Reprinted*, vol. 3, no. 2, pp.81-101, 1948.
[45] S. Singer, "Gyrators application in power processing circuits," *IEEE Transactions on Industrial Electronics*, vol. IE-34, no. 3, pp. 313-318, 1987.
[46] G. Pillonnet, "Modeling and efficiency analysis of multiphase resonant-switched capacitive converters," *IEEE Transactions on Power Electronics*, vol. 31, no. 1, pp. 11-14, 2016.
[47] D. Shmilovitz, "Gyrator Realization Based on a Capacitive Switched Cell," in *IEEE Transactions on Circuits and Systems II: Express Briefs*, vol. 53, no. 12, pp. 1418-1422, 2006.
[48] Y.-H. Liu, S.-C. Wang and Y.-F. Luo, "Digital dimming control of CCFL drive system using pulse density modulation technique," *IEEE Region 10 Conference,* pp. 1-4, 2007.
[49] X. Zhang, Y. Pu, K. Ishida, Y. Ryu, Y. Okuma, P.-H. Chen, K. Watanabe, T. Sakurai, and M. Takamiya, "A 1-V-input switched-capacitor voltage converter with voltage-reference-free pulse-density modulation," *IEEE Transactions on Circuits and Systems II: Express Briefs*, vol. 59, no. 6, pp. 361-365, 2012.
[50] A. Cervera and M. M. Peretz, "Envelope tracking power supply for volume-sensitive low-power applications based on a resonant switched-capacitor converter," *IEEE Applied Power Electronics Conference and Exposition*, pp. 2298-2303, 2016.
[51] O. Kirshenboim, A. Cervera, M. M. Peretz, "Improving loading and unloading transient response of a voltage regulator module using a load-side auxiliary gyrator circuit", *IEEE Transactions on Power Electronics*, *Early Access,* vol. PP, no. 99, pp.1-1, 2016